

Single-electron second-order correlation function $G^{(2)}$ at nonzero temperatures

Michael Moskalets*

Department of Metal and Semiconductor Physics, NTU Kharkiv Polytechnic Institute, 61002 Kharkiv, Ukraine

(Received 31 May 2018; revised manuscript received 3 August 2018; published 11 September 2018)

The single-particle state is not expected to demonstrate second-order coherence. Here I analyze the injection of electrons into a conductor and show that, at a nonzero temperature, the underlying Fermi sea causes the single-particle injected state to exhibit second-order coherence. For this purpose, I calculate the second-order correlation function, $G^{(2)}$, of electrons injected on top of the Fermi sea. At zero temperature, the function $G^{(2)}$ unambiguously demonstrates whether the injected state is a single- or a multiparticle state: $G^{(2)}$ vanishes in the former case, while it does not vanish in the latter case. However, at nonzero temperatures, when the injected state is a mixed state, a purely single-particle contribution makes the function $G^{(2)}$ nonvanishing even in the case of injection of one electron. The single-particle contribution puts the lower limit on the second-order correlation function and thereby limits its use as a single-particle injection test at nonzero temperatures. The existence of a single-particle contribution to $G^{(2)}$ can be verified experimentally by measuring the cross-correlation electrical noise.

DOI: [10.1103/PhysRevB.98.115421](https://doi.org/10.1103/PhysRevB.98.115421)**I. INTRODUCTION**

Quantum coherent electronics [1,2], also known as electron quantum optics [3], and single-electron electronics [4], is an actively developing platform for quantum information processing [5], which is aimed at creating, manipulating, and detecting individual electrons as carriers of information.

Recently, quite a lot of single-electron sources on-demand have been experimentally realized [6–17]. One of the crucial tests this source has to pass through is the verification of a single-particle emission regime.

In quantum optics, the single-photon emission regime is verified via the measurement of the second-order correlation function, $g^{(2)}$, which characterizes the probability of joint detection of two photons [18]. Such a verification is universal and it does not rely on any specific properties of the source. If the stream generated by a periodically working source consists of nonoverlapping single photons, then the function $g^{(2)}(\tau)$ vanishes at zero time delay between the two detections, $\tau = 0$. In contrast, if there are multiphoton wave packets in the stream, the two photons can be detected simultaneously and the function $g^{(2)}$ is finite at $\tau = 0$.

The measurement of the joint detection probability in the optical frequencies range is possible due to availability of efficient single photon detectors. In the microwave frequencies range, no efficient detectors are available. Nevertheless, the single-particle emission regime for a source of microwave photons [19] can be demonstrated via the linear amplification of the magnitude of an electromagnetic field [20].

There are no efficient on-fly detectors available for single electrons so far, and there is no way to measure the magnitude of a fermionic field. This is why for the verification of a single-electron emission regime, the various nonuniversal methods

were used. The nonuniversality in this context means that the given method can be good for one system, but not for another. In particular, a strong decrease in an electrical noise was used as an indicator of the single-particle emission regime for a dynamical quantum dot [21] and for a quantum capacitor [22–24], while this method does not work in the case of the source of levitons [11]. Another method for validation of the single-electron injection regime, which relies on the partition noise [25,26] of an electron beam splitter, was demonstrated in Refs. [11,27].

Nevertheless, in some systems it is possible to measure directly the second-order correlation function for injected electrons, $G^{(2)}$, which vanishes identically in the case of a single-particle injection. Generally, in the case of electrons injected into an electron waveguide, the second-order correlation function contains several contributions: (i) One is due to electrons belonging to the Fermi sea of the waveguide, (ii) one more is due to the injected electrons, that is $G^{(2)}$, (iii) and, finally, the last contribution is due to the joint contribution of the injected electrons and Fermi-sea electrons [28–30]. As it is pointed out in Ref. [29], when electrons are injected into one of the two incoming channels of an electron beam splitter, the cross-correlation noise of currents after the beam splitter is directly related to the function $G^{(2)}$. The Fermi sea electrons do not contribute to the cross-correlation noise either directly or in conjunction with injected electrons. For this to be true, the two conditions must be met. First, the Fermi seas in both incoming channels have the same temperature and the same chemical potential. Second, the incoming and outgoing channels are spatially separated, which can be achieved using chiral or helical edge states [31] as electron waveguides.

Here I focus on the effect of temperature on the second-order correlation function, $G^{(2)}$, of electrons injected on top of the Fermi sea in conductors. The fact that at nonzero temperatures the quantum state of injected electrons is a mixed

*michael.moskalets@gmail.com

state, [32,33] leads to existence of a purely single-particle contribution to the correlation function $G^{(2)}$. This contribution puts the lower limit to the second-order correlation function, and it must be taken into account when the function $G^{(2)}$ is used to distinguish single-electron and multielectron injected quantum states.

The paper is organized as follows: In Sec. II, I discuss the effect of temperature on the correlation function $G^{(2)}$ of electrons injected on top of the Fermi sea. In Sec. III, the relation between the function $G^{(2)}$ and the current correlation function is given in frequency domain. The temperature dependence of the functions $G^{(2)}$ for single- and two-electron excitations are contrasted in Sec. IV. The conclusion is given in Sec. V. Some details of calculations are presented in Appendixes A and B.

II. CORRELATION FUNCTION OF ELECTRONS INJECTED AT NONZERO TEMPERATURES

If the single-electron source injects particles with an energy close to the Fermi energy of the electrons in the conductor, the injected quantum state becomes temperature dependent [33]. The relevant sources are, for example, the source of levitons [11], and a source based on a quantum capacitor [7,34,35] in a regime that is described by a model of a single quantum level raising at a constant rapidity [36]. Namely, these sources are assumed below.

The first-order coherence of injected electrons is conveniently characterized by the excess first-order correlation function, $G^{(1)}$ [37–39]. To get rid of the contribution of the underlying Fermi sea and keep track of the contribution of injected electrons only, this function is defined as the difference of the two terms, evaluated with the source being switched on and off, respectively, $G^{(1)}(1; 2) = \langle \hat{\Psi}^\dagger(1)\hat{\Psi}(2) \rangle_{\text{on}} - \langle \hat{\Psi}^\dagger(1)\hat{\Psi}(2) \rangle_{\text{off}}$. Here $\hat{\Psi}(j)$ is an electron field operator in second quantization evaluated at time t_j and point x_j , $j = 1, 2$, behind the source. The effect of a working source is encoded in these operators. The quantum statistical average, $\langle \dots \rangle$, is performed over the equilibrium state of electrons in the conductor to which the waveguide is connected. This state is characterized by the Fermi distribution function with a temperature θ and a chemical potential μ . In this paper, I suppose that the waveguide is a chiral one-dimensional conductor. Since I am interested in time dependence rather than spatial dependence, below, I only keep the argument t_j .

The excess first-order correlation function is experimentally accessible. For instance, the function $G^{(1)}$ for a stream of identically prepared separated electrons in a ballistic conductor was measured in Ref. [40] using the tomography protocol suggested in Ref. [38].

On the contrary, the second-order coherence of injected electrons is more difficult to access. The total second-order correlation function is defined as follows, $\mathcal{G}^{(2)}(t_1, t_2; t_3, t_4) = \langle \hat{\Psi}^\dagger(t_1)\hat{\Psi}^\dagger(t_2)\hat{\Psi}(t_3)\hat{\Psi}(t_4) \rangle$ [28,29]. For the Fermi sea of noninteracting electrons of interest here, this function is calculated as the 2×2 Slater determinant composed of $\mathcal{G}^{(1)}(t_1; t_2) = \langle \hat{\Psi}^\dagger(t_1)\hat{\Psi}(t_2) \rangle$ taken with corresponding arguments.

When the source is on, this function, $\mathcal{G}_{\text{on}}^{(2)}$, which characterizes the second-order coherence of the Fermi sea together

with injected electrons, contains three distinct contributions [28,29]. One of them is of particular interest; it is due to electrons injected by the source. This contribution, which I denote as $G^{(2)}$, is composed of excess first-order correlation functions, $G^{(1)}$, in the very same way as the total $\mathcal{G}^{(2)}$ is composed of the total $\mathcal{G}^{(1)}$:

$$G^{(2)}(t_1, t_2; t_3, t_4) = \det \begin{pmatrix} G^{(1)}(t_1; t_4) & G^{(1)}(t_1; t_3) \\ G^{(1)}(t_2; t_4) & G^{(1)}(t_2; t_3) \end{pmatrix}. \quad (1)$$

Another contribution is due to electrons belonging to the Fermi sea of a waveguide. This contribution can be calculated with the source turned off, $\mathcal{G}_{\text{off}}^{(2)}$. This contribution characterizes the second-order coherence of the Fermi sea alone. Yet another contribution is due the joint effect of injected electrons and electrons belonging to the Fermi sea of a waveguide. It is this last contribution which prevents us from determining $G^{(2)}$ as the excess $\mathcal{G}^{(2)}$, that is, $G^{(2)} \neq \mathcal{G}_{\text{on}}^{(2)} - \mathcal{G}_{\text{off}}^{(2)}$. Nevertheless, as it was argued in Ref. [29], the function $G^{(2)}$ can be accessed directly through the cross-correlation noise. Since $G^{(2)}$ is experimentally accessible, one can use it to characterize the second-order coherence of injected electrons. Below, I discuss in detail the properties of $G^{(2)}$.

First consider injection at zero temperature, when the injected particles are in a pure quantum state. For a single-particle state ($N = 1$) with wave function $\Psi_1(t)$, the first-order correlation function is factorized into the product of two terms that depend on one time each, $G_{N=1}^{(1)}(t_1; t_2) = \Psi_1^*(t_1)\Psi_1(t_2)$ [33,41]. Apparently, that in this case the second-order correlation function vanishes identically, $G_{N=1}^{(2)} = 0$. However, already for a two-particle state ($N = 2$), when $G_{N=2}^{(1)}(t_1; t_2) = \sum_{j=1}^2 \Psi_j^*(t_1)\Psi_j(t_2)$, the second-order correlation function is not zero. It is represented as follows, $G_{N=2}^{(2)}(t_1, t_2; t_3, t_4) = \Psi_{1,2}^{(2)*}(t_1, t_2)\Psi_{1,2}^{(2)}(t_3, t_4)$, where the two-particle wave function,

$$\Psi_{1,2}^{(2)}(t_1, t_2) = \det \begin{pmatrix} \Psi_1(t_1) & \Psi_2(t_1) \\ \Psi_1(t_2) & \Psi_2(t_2) \end{pmatrix}, \quad (2)$$

is the Slater determinant composed of wave functions of both particles, Ψ_1 and Ψ_2 .

In contrast, at nonzero temperatures, the electrons injected by the source on top of the Fermi sea are in a mixed quantum state. In the case of a two-particle state, the first-order correlation function reads [33,41]

$$G_{N=2}^{(1)}(t_1; t_2) = \int d\epsilon p_\theta(\epsilon) \sum_{j=1}^2 \Psi_{j\epsilon}^*(t_1)\Psi_{j\epsilon}(t_2), \quad (3)$$

where the index j labels the mixed state of one of the two particles, $j = 1, 2$. The components of such a mixed state are parametrized by a continuous variable, the energy ϵ , with the probability density $p_\theta(\epsilon) = -\partial f(\epsilon)/\partial \epsilon$, where $f(\epsilon) = (1 + e^{\frac{\epsilon - \mu}{k_B \theta}})^{-1}$ is the Fermi distribution function, k_B is the Boltzmann constant, and ϵ is the energy counted from the Fermi energy, $\epsilon = E - \mu$, cf. the Fermi function definition after Eq. (A4).

Accordingly, to Eq. (1), the second-order correlation function becomes

$$G_{N=2}^{(2)}(t_1, t_2; t_3, t_4) = \int d\epsilon p_\theta(\epsilon) \int d\epsilon' p_\theta(\epsilon') \left\{ \Psi_{1\epsilon, 2\epsilon'}^{(2)*}(t_1, t_2) \Psi_{1\epsilon, 2\epsilon'}^{(2)}(t_4, t_3) + \sum_{j=1}^2 \Psi_{j\epsilon, j\epsilon'}^*(t_1, t_2) \Psi_{j\epsilon, j\epsilon'}(t_4, t_3) \right\}. \quad (4)$$

Here the two-particle wave function $\Psi_{1\epsilon, 2\epsilon'}^{(2)}$ is determined by Eq. (2) with Ψ_1 being replaced by $\Psi_{1\epsilon}$ and Ψ_2 being replaced by $\Psi_{2\epsilon'}$. In addition, we have a new function $\Psi_{j\epsilon, j\epsilon'}$ dependent of two times, which is determined by the Slater determinant composed of different components of the same single-particle mixed state,

$$\Psi_{j\epsilon, j\epsilon'}(t_1, t_2) = \frac{1}{\sqrt{2}} \det \begin{pmatrix} \Psi_{j\epsilon}(t_1) & \Psi_{j\epsilon'}(t_1) \\ \Psi_{j\epsilon}(t_2) & \Psi_{j\epsilon'}(t_2) \end{pmatrix}. \quad (5)$$

I name it *the two-time wave function*. Note that at coincident times, $t_1 = t_2$, this function is zero, $\Psi_{j\epsilon, j\epsilon'}(t, t) = 0$, which is a manifestation of the fermionic nature of an electron.

The contribution to $G^{(2)}$ due to the two-time wave function is present even in the case when $N = 1$ (that is, $j = 1$) in Eq. (3). The corresponding state I call *a single-particle mixed state* with components described by the single-particle correlation functions $G_{1\epsilon}^{(1)}(t_1; t_2) = \Psi_{1\epsilon}^*(t_1) \Psi_{1\epsilon}(t_2)$ appeared with probability $p_\theta(\epsilon)$. Single particle means here that only one component of the mixed state appears at a time. Therefore, the number of particles described by this mixed state does not fluctuate and is equal to one. The interpretation that only one component of the mixed state appears at a time is in line with the interpretation of the state of a finite-temperature Fermi sea into which a particle is injected, see Eq.(7) in Ref. [42]. According to that interpretation, the quantum state of the Fermi sea at nonzero temperature can be represented as the mixed state, whose components are the Fermi seas with zero temperature, completely filled up to the energy $\mu + \epsilon$, which appear one at a time with probability $p_\theta(\epsilon)$.

So, for $N = 1$, Eq. (4) becomes

$$G_{N=1}^{(2)}(t_1, t_2; t_3, t_4) = \int d\epsilon p_\theta(\epsilon) \int d\epsilon' p_\theta(\epsilon') \times \Psi_{1\epsilon, 1\epsilon'}^*(t_1, t_2) \Psi_{1\epsilon, 1\epsilon'}(t_4, t_3). \quad (6)$$

Note, at zero temperature, $\theta = 0$, the probability density becomes the delta function of energy, $p_\theta(\epsilon) = \delta(\epsilon - \mu)$, and the only component with Fermi energy, $\epsilon = \mu$, survives. Since $\Psi_{j\mu, j\mu}(t_1, t_2) = 0$, the second-order correlation function vanishes at zero temperature, $G_{N=1}^{(2)} = 0$, as expected for a single-particle state. In contrast, at nonzero temperatures, $\theta > 0$, when $p_\theta(\epsilon) \neq \delta(\epsilon - \mu)$, a single-particle state demonstrates some degree of second-order coherence, which is quantified by $G_{N=1}^{(2)} \neq 0$.

This is somewhat counterintuitive, since the quantities like $G^{(2)}$ are considered essentially multiparticle in nature. Indeed, in the case of a pure state, $G^{(2)}(t_1, t_2; t_2, t_1) = |\Psi^{(2)}(t_1, t_2)|^2$. The conventional meaning of the wave function square is the detection probability, the probability of a strong, projective

measurement. In our case, it is the joint probability of two detections, at time t_1 and at time t_2 .

In the case of a two-particle state, say, with wave functions $\Psi_1(t)$ and $\Psi_2(t)$, both detections are possible. Let us suppose that in the first measurement we detect a particle with wave function Ψ_1 at time $t = t_1$. The projective measurement means that, after the detection, the wave function is collapsed; it is reduced to the delta function, $\Psi_1(t) \sim \delta(t - t_1)$. Therefore, the original wave function cannot be measured at any other times. However, there is a second particle with wave function $\Psi_2(t)$, which can be detected in the second measurement, say, at time $t = t_2 \neq t_1$. Hence, we are able to perform two measurements, and the probability for such a joint measurement is given by $G_{N=2}^{(2)}(t_1, t_2; t_2, t_1) \neq 0$.

In the case of a single-particle state, we can perform a projective measurement only once, say, at $t = t_1$, and cannot measure the same state again $t = t_2 \neq t_1$. This fact is manifested as $G_{N=1}^{(2)} = 0$, which works perfectly well in the case of injection at zero temperature.

However, in the case of injection at nonzero temperatures, this logic seems to fail, $G_{N=1}^{(2)} \neq 0$, see Eq. (6) for $\theta > 0$. To resolve this seeming paradox, let's remember that a classical (nonquantum) particle can be measured as many times as we need. Therefore, one can say that the Fermi sea at nonzero temperatures causes an injected particle to behave classically and to exhibit the second-order coherence.

A direct reading of Eq. (6) with $t_4 = t_1$ and $t_3 = t_2$ suggests that a possible mechanism that would explain why a particle in a mixed state would behave classically, that is, could be measured more than once, is as follows. A particle in a mixed state can be in several quantum states, components of the mixed state, appearing with some probabilities. In Eqs. (6) and (5), these states are $\Psi_{1\epsilon}$ for various ϵ . When we detect a particle at time $t = t_1$, we detect it in some particular component state, say, in the state with $\epsilon = \epsilon_0$. As a result, this component is reduced to the delta function, $\Psi_{1\epsilon_0}(t) \sim \delta(t - t_1)$, and, therefore, cannot be measured at any other times. But there are many other components of the mixed state with $\epsilon' \neq \epsilon_0$. Any of them is available for the next detection, say, at time $t = t_2 \neq t_1$.

The ability of a single-particle state injected at nonzero temperature to demonstrate the second-order coherence can be verified (or refuted) experimentally.

III. $G^{(2)}$ AND THE CROSS-CORRELATION NOISE

As it was pointed-out in Ref. [29], the second-order correlation function with pairwise equal arguments, $G^{(2)}(t_1, t_2; t_2, t_1)$, is directly related to the cross-correlation symmetrized noise [43–46]. More precisely, it is related to the currents, $I_3(t_1)$ and $I_4(t_2)$, and their correlation function, $P_{34}(t_1, t_2)$, which are measured at the outputs of an electronic interferometer [47–49], analogous to the Hanbury Brown and Twiss (HBT) interferometer [50] known in optics, see Fig. 1. The source of electrons is placed in one of the inputs. The temperature of both input channels 1 and 2, with and without an electron source, should be the same, $\theta_1 = \theta_2 \equiv \theta$. Since the source injects particles periodically with period \mathcal{T}_0 , the

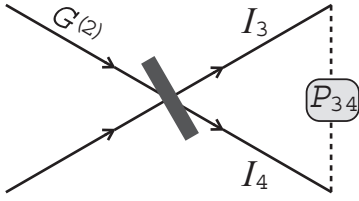


FIG. 1. Scheme of an electron HBT interferometer, where the quantum state injected into one of the input channels (marked by $G^{(2)}$) is transmitted through and reflected at the wave splitter (shown as a shaded thin rectangle). As a result, the outgoing current I_3 and I_4 are generated. These currents, together with their cross-correlation function P_{34} , define the second-order correlation function of injected state, $G^{(2)}$, according to Eq. (9). The arrows show the direction of propagation of electrons.

resulting currents are periodic functions of time, $I_\alpha(t) = I_\alpha(t + \mathcal{T}_0)$, $\alpha = 3, 4$.

Since the measurement of a time-resolved noise is challenging, below I focus on a frequency-resolved noise [51–57], which was measured more than once, see, e.g., Refs. [58–60] and also Ref. [22], where, as I already mentioned, a frequency-resolved noise was used for validation of the single-electron injection regime.

Let us introduce the following Fourier transform:

$$G_\ell^{(2)}(\omega) = \int_0^{\mathcal{T}_0} dt e^{i\Omega\ell t} \int_{-\infty}^{\infty} d\tau e^{i\omega\tau} G^{(2)}(t + \tau, t; t, t + \tau), \quad (7)$$

where $\Omega = 2\pi/\mathcal{T}_0$ and ℓ is an integer. Then, $G_\ell^{(2)}(\omega)$ is expressed in terms of the finite-frequency cross-correlation noise power, $\mathcal{P}_{34,\ell}(\omega)$ and outgoing currents I_3 and I_4 , as follows (see Appendix A for the precise definition of $\mathcal{P}_{34,\ell}(\omega)$, Eqs. (A3) and (A4), and for the corresponding derivation within the Floquet scattering matrix approach):

$$v_\mu^2 G_\ell^{(2)}(\omega) = \frac{\mathcal{P}_{34,\ell}(\omega)}{e^2 RT/\mathcal{T}_0} + \frac{1}{e^2 RT} \int_0^{\mathcal{T}_0} e^{i\Omega\ell t} dt \int_{-\infty}^{\infty} d\tau e^{i\omega\tau} I_3(t + \tau) I_4(t). \quad (8)$$

Here T and $R = 1 - T$ are the transmission and reflection probabilities of a wave splitter of an electron HBT interferometer, v_μ is the Fermi velocity of electrons in a waveguide, e is an electron charge.

In the special case, when the excitations produced during different periods do not overlap, Eq. (8) can be simplified. We take into account explicitly the fact that the current is periodic, set $\mathcal{T}_0 \rightarrow \infty$, and introduce a continuous frequency $\omega_\ell = \ell\Omega$ instead of the series of discrete frequencies $\ell\Omega$, see Appendix A 4 for details. Then Eq. (8) becomes

$$v_\mu^2 G_\ell^{(2)}(\omega) = \frac{\mathcal{P}_{34,\ell}(\omega)}{e^2 RT/\mathcal{T}_0} + \frac{I_3(\omega) I_4(\omega_\ell - \omega)}{e^2 RT/\mathcal{T}_0^2}. \quad (9)$$

This equation resembles Eq. (22) of Ref. [28], where the two-energy distribution function was related to the zero-frequency noise power and DC currents in the circuit with two energy

filters, quantum dots each with one working resonant quantum level.

Below, I will use Eq. (9) and address the temperature dependence of $G_\ell^{(2)}(\omega)$ for electrons injected by some particular source, namely the source of levitons [11], that is capable of generating single- as well as few-particle excitations [61–66]. The aim is to find out whether the function $G^{(2)}$ in frequency representation can uniquely distinguish a single-particle state from a multiparticle state, with accounting for a multiparticlelike behavior of a single-particle state at nonzero temperatures. As can be seen from the example below, this is not always possible if only one set of frequencies is available. Measuring on multiple frequency sets can increase confidence. However, only $G^{(2)}$ in the time domain can do this job with full certainty.

IV. EXAMPLE: THE SOURCE OF LEVITONS

The sequence of the Lorentzian voltage pulses,

$$eV(t) = N \sum_{m=-\infty}^{\infty} \frac{2\hbar\Gamma_\tau}{(t - m\mathcal{T}_0)^2 + \Gamma_\tau^2}, \quad (10)$$

applied to a metallic contact, generates the stream of excitations with charge eN each in a ballistic channel attached to the contact [67–69]. Here Γ_τ is the half-width of a voltage pulse. These excitations are named N -electron levitons or N -levitons [70].

A. Correlation functions

In the regime, when the period is much larger than the width of a voltage pulse, $\mathcal{T}_0 \gg \Gamma_\tau$, the excitations created at different periods do not overlap. Then, we can restrict ourselves to a single period only, say, $m = 0$, and send $\mathcal{T}_0 \rightarrow \infty$ in the integrals we need to evaluate. In this case, the first-order correlation function of excitations injected by the source of levitons is represented as follows:

$$G^{(1)}(t_1; t_2) = \int d\epsilon p_\theta(\epsilon) \sum_{j=1}^N \Psi_{j,\epsilon}^*(t_1) \Psi_{j,\epsilon}(t_2). \quad (11)$$

Here $\Psi_{j,\epsilon}(t) = e^{-it\frac{\epsilon+\epsilon}{\hbar}} \psi_j(t)$ is the wave function of the j th particles comprising an N -electron leviton ($j = 1, \dots, N$). The corresponding envelope function is the following [71–73]:

$$\psi_j(t) = \sqrt{\frac{\Gamma_\tau}{\pi v_\mu}} \frac{1}{t - i\Gamma_\tau} \left(\frac{t + i\Gamma_\tau}{t - i\Gamma_\tau} \right)^{j-1}. \quad (12)$$

Using the fact that the envelope wave functions, ψ_j , are independent of energy, we can integrate ϵ out in Eq. (11) and get

$$G^{(1)}(t_1; t_2) = \eta \left(\frac{t_1 - t_2}{\tau_\theta} \right) \sum_{j=1}^N \psi_j^*(t_1) \psi_j(t_2), \quad (13)$$

where $\eta(x) = x/\sinh(x)$ and the thermal coherence time is $\tau_\theta = \hbar/(\pi k_B \theta)$.

Substituting the above equation into Eq. (1), one can calculate the second-order correlations function. For $t_1 = t_4$

and $t_2 = t_3$ we have

$$G^{(2)}(t_1, t_2; t_2, t_1) = \sum_{j=1}^N \sum_{k=1}^N \left\{ |\psi_j(t_1)|^2 |\psi_k(t_2)|^2 - \eta^2 \left(\frac{t_1 - t_2}{\tau_\theta} \right) \psi_j^*(t_1) \psi_j(t_2) \psi_k^*(t_2) \psi_k(t_1) \right\}. \quad (14)$$

Now I will analyze the above equation in two cases, $N = 1$ and $N = 2$.

B. A single-electron leviton, $N = 1$

For a single-particle leviton, $N = 1$, the function $G^{(2)}$ becomes

$$v_\mu^2 G_{N=1}^{(2)}(t_1, t_2; t_2, t_1) = \frac{\Gamma_\tau^2}{\pi^2} \frac{1 - \eta^2 \left(\frac{t_1 - t_2}{\tau_\theta} \right)}{(t_1^2 + \Gamma_\tau^2)(t_2^2 + \Gamma_\tau^2)}. \quad (15)$$

From this equation, we can conclude the following. First, when the time difference is smaller than the thermal coherence time, $|t_1 - t_2| \ll \tau_\theta$, the function $\eta = 1$, and the second-order correlation function vanishes, $G_{N=1}^{(2)} = 0$. This fact is a manifestation of a single-particle nature of a quantum state in question.

Second, at larger time difference, $|t_1 - t_2| \gg \tau_\theta$, the function $\eta \rightarrow 0$, and the second order correlation function is factorized into the product of two terms, each of which depends only on one time, $G_{N=1}^{(2)}(t_1, t_2; t_2, t_1) = |\psi_1(t_1)|^2 |\psi_1(t_2)|^2$. Namely, the two-particle detection probability becomes the product of two statistically independent single-particle detection probabilities. Such a property is expected for a classical rather than a quantum state.

Nevertheless, the state of a leviton remains quantum and respects the Pauli exclusion principle, which requires that the function $G^{(2)}$ strictly vanishes at equal times (at any temperature), $G_{N=1}^{(2)}(t, t; t, t) = 0$.

The frequency representation

Let us perform the Fourier transformation defined in Eq. (7) on the function $G^{(2)}$ of a single leviton, Eq. (15). Using the fact that $\mathcal{T}_0 \gg \Gamma_\tau$, we get

$$v_\mu^2 G_{N=1, \ell}^{(2)}(\omega) = e^{-|\omega|\Gamma_\tau} e^{-|\omega - \omega_\ell|\Gamma_\tau} - e^{-|\omega_\ell|\Gamma_\tau} \times \frac{\Gamma_\tau}{\pi} \int_{-\infty}^{\infty} d\tau \frac{\eta^2 \left(\frac{\tau}{\tau_\theta} \right)}{\tau^2 + 4\Gamma_\tau^2} \left\{ \cos(\omega\tau) + \cos([\omega - \omega_\ell]\tau) + \frac{2\Gamma_\tau}{\tau} \text{sgn}(\omega_\ell) [\sin(\omega\tau) - \sin([\omega - \omega_\ell]\tau)] \right\}. \quad (16)$$

As I already mentioned, this function is experimentally accessible through the finite-frequency noise measurement, see Eq. (9).

In Fig. 2, I show $G_{N=1, \ell}^{(2)}(\omega)$, Eq. (16), as a function of temperature for several fixed frequencies. The set of frequencies chosen aims to illustrate various ways how noise can approach zero with decreasing temperature. This is important

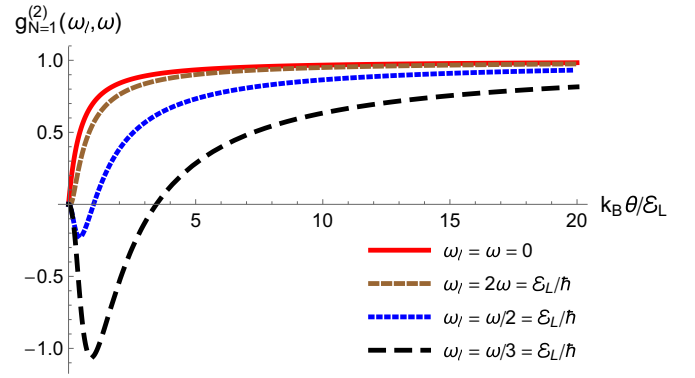


FIG. 2. The second-order correlation function of a single leviton, Eq. (16), normalized to its high-temperature asymptotics, $g_{N=1}^{(2)}(\omega_\ell, \omega) = v_\mu^2 G_{N=1, \ell}^{(2)}(\omega) / (e^{-|\omega|\Gamma_\tau} e^{-|\omega - \omega_\ell|\Gamma_\tau})$, is given as a function of temperature. The temperature, $k_B \theta$, and frequencies, $\hbar \omega$ and $\hbar \omega_\ell$, are given in units of the energy of a leviton, $\mathcal{E}_L = \hbar / (2\Gamma_\tau)$.

to be aware of, if measurement is only available with a fixed frequency.

At strictly zero temperature, $G_{N=1, \ell}^{(2)}(\omega) = 0$ for any frequencies, demonstrating that the state in question is a genuine single-particle state. At nonzero temperatures, the function $G^{(2)}$ deviates from zero. It can first become positive, the two upper lines in Fig. 2, or, first negative, and then positive, the two lower lines in Fig. 2.

At high temperatures, when the thermal coherence time becomes smaller than the width of a voltage pulse, $\tau_\theta \ll \Gamma_\tau$, the second-order correlation function achieves its high-temperature asymptotic behavior, $v_\mu^2 \lim_{\theta \rightarrow \infty} G_{N=1, \ell}^{(2)}(\omega) = e^{-|\omega|\Gamma_\tau} e^{-|\omega - \omega_\ell|\Gamma_\tau}$. This product form is characteristic of the classical state.

Note, that the growth of $G_{N=1}^{(2)}$ with temperature is also manifested in the reduction of a single-particle shot noise [32,42,61], the effect that has already been measured in Refs. [3,27,74,75].

The temperature dependence of the function $G^{(2)}$ for a multielectron state is remarkably different. Namely, its zero temperature limit is not universal. On the contrary, such a limit depends strongly on frequency. To illustrate this statement, let us consider the case of a two-electron leviton.

C. A two-electron leviton, $N = 2$

The correlation function of a two-electron leviton, $G_{N=2, \ell}^{(2)}$, is given in Eq. (11) with $N = 2$. The corresponding wave functions are presented in Eq. (12). After performing the Fourier transformation, according to Eq. (7), we obtain $G_{N=2, \ell}^{(2)}(\omega)$, see Eq. (B4), which is shown in Fig. 3 as a function of temperature for several fixed frequencies.

We can see that at zero temperature, the magnitude of $G_{N=2, \ell}^{(2)}(\omega)$ is not zero, unlike the case of a plain leviton, $N = 1$. Indeed, it strongly depends on the frequencies ω_ℓ and ω . Such a nonuniversal frequency-dependent behavior is characteristic of a multiparticle state, the two-particle state in the present case.

Moreover, at some frequencies by chance, see the blue dashed line in Fig. 3, the function $G^{(2)}$ can approach zero

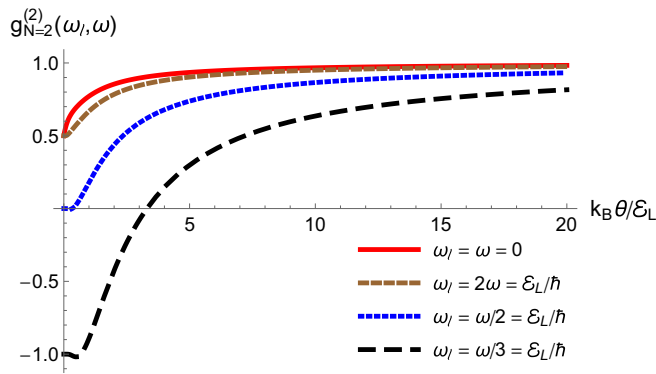


FIG. 3. The second-order correlation function of a two-electron leviton, Eq. (B4), normalized to its high-temperature asymptotics, $g_{N=2}^{(2)}(\omega_\ell, \omega) = v_\mu^2 G_{N=2,\ell}^{(2)}(\omega)/[4e^{-|\omega|\Gamma_\tau} e^{-|\omega-\omega_\ell|\Gamma_\tau}]$, is given as a function of temperature. The temperature, $k_B\theta$, and frequencies, $\hbar\omega$ and $\hbar\omega_\ell$, are given in units of the energy of a leviton, $\mathcal{E}_L = \hbar/(2\Gamma_\tau)$.

with decreasing temperature. This fact can be misinterpreted as an indication of a single-particle state. To avoid this, measurements at several frequencies are desirable.

Interestingly, the high-temperature asymptotics of the second-order correlation function of a multielectron leviton is universal: It is determined by the corresponding asymptotics of the function $G^{(2)}$ of a single-electron leviton,

$$\lim_{\theta \rightarrow \infty} G_{N=N_0}^{(2)} = N_0^2 \lim_{\theta \rightarrow \infty} G_{N=1}^{(2)}. \quad (17)$$

This is a manifestation of the high-temperature fusion effect (when the multielectron system behaves like one particle of the total charge) discussed in Ref. [41].

Note that the low-temperature regime, for which Figs. 2 and 3 show different behavior, is achievable in present day experiment. So, in Ref. [74], the voltage pulses with width $2\Gamma_\tau = 75$ ps were used to generate levitons with energy $\mathcal{E}_L \approx 320$ mK. The experimental data on shot noise were reported for the temperature range from $\theta_1 = 40$ mK to $\theta_2 = 138$ mK. Correspondingly, the ratio θ/\mathcal{E}_L is changed from $\theta_1/\mathcal{E}_L \approx 0.125$ to $\theta_2/\mathcal{E}_L \approx 0.43$. From Figs. 2 and 3, we see that for these parameters the function $G^{(2)}$ allows one to uniquely distinguish single-particle and multiparticle states: The second-order correlation function, $G^{(2)}$, is almost constant in the case of a two-electron leviton, while it decreases rapidly to zero with decreasing temperature in the case of a single-electron leviton.

V. CONCLUSION

I have discussed the effect of temperature on the second-order correlation function of electrons, $G^{(2)}$, which are injected by an on-demand source on top of the Fermi sea in a conductor.

The second-order correlation function is a universal tool that is able to distinguish between single- and multiparticle injection regime of an electron source. The function $G^{(2)}$ is accessible via the cross-correlation electrical noise measurement at the exit of an electron Hanbury Brown and Twiss interferometer.

At zero temperature, the function $G^{(2)}$ is vanishing in the case of a single-electron injection and does not vanish in the case of multiparticle injection. In contrast, at nonzero temperatures, the function $G^{(2)}$ does not vanish even in the case of a single-electron injection. The reason is that at nonzero temperatures, the single-particle quantum state is a mixed state that demonstrates some degree of second-order coherence, which is quantified by $G^{(2)} \neq 0$. The existence of this single-particle contribution has to be taken into account, when the second-order correlation function is used for the verification of a single-particle injection into conductors at nonzero temperatures.

ACKNOWLEDGMENTS

I appreciate the warm hospitality of the Department of Applied Physics, Aalto University, Finland, where this project was started. I am grateful to Christian Flindt and Pablo Buset for numerous discussions.

APPENDIX A: ELECTRON VERSUS ELECTRICAL CORRELATION FUNCTIONS

The setup of interest consists of an electron wave splitter, a quantum point contact [76,77], with two incoming, $\alpha = 1, 2$, and two outgoing, $\beta = 3, 4$, one-dimensional waveguides, which are connected to respective metallic leads with the same temperature θ and chemical potential μ , see Fig. 1. The transmission T and reflection $R = 1 - T$ probabilities of a wave splitter are energy independent (within the energy range relevant to our problem).

One of the incoming waveguides, say $\alpha = 1$, is connected to an electron source that periodically emits particles. The period is denoted as \mathcal{T}_0 . Within the scattering approach, the periodically working source is characterized by the Floquet scattering matrix S_F dependent on two energies, E and $E_n = E + n\hbar\Omega$ with n being integer and the frequency $\Omega = 2\pi/\mathcal{T}_0$ is dictated by the periodicity. By the virtue of definition, $S_F(E_n, E)$ is a quantum-mechanical amplitude for the process, when an electron with energy E passing by a source changes its energy to E_n [78].

My aim here is to prove Eq. (8). For this, I use Eq. (1) and write

$$G^{(2)}(t_1, t_2; t_2, t_1) = -|G^{(1)}(t_1; t_2)|^2 + G^{(1)}(t_1; t_1)G^{(1)}(t_2; t_2). \quad (A1)$$

The first-order correlation function at coincident times defines an electrical current generated by the source, $I(t) = ev_\mu G^{(1)}(t; t)$ [79]. The outgoing currents are expressed in terms of the incoming current $I(t)$, as follows, $I_3(t) = RI(t)$ and $I_4(t) = TI(t)$. The currents are periodic in time, $I(t) = I(t + \mathcal{T}_0)$. Therefore, after the Fourier transform defined in Eq. (7), the second line of Eq. (A1) reproduces the second line of Eq. (8).

To prove that the first term on the right-hand side of Eq. (A1) leads to the first term on the right-hand side of Eq. (8), I express both the cross-correlation electrical noise power of the outgoing currents, \mathcal{P}_{34} , and the excess first-order correlation function of electrons injected by the source, $G^{(1)}$,

in terms of the Floquet scattering matrix of the source, and then relate them to each other.

1. Frequency-dependent electrical noise

The symmetrized cross-correlation function of electrical currents I_3 and I_4 flowing out of the wave splitter, see Fig. 1, is defined as follows [80]:

$$P_{34}(t_1, t_2) = \frac{1}{2} \langle \Delta \hat{I}_3(t) \Delta \hat{I}_4(t + \tau) + \Delta \hat{I}_4(t + \tau) \Delta \hat{I}_3(t) \rangle, \quad (\text{A2})$$

where $\Delta \hat{I}_\alpha(t) = \hat{I}_\alpha(t) - \langle \hat{I}_\alpha(t) \rangle$, $\alpha = 3, 4$, is an operator of current fluctuations in second quantization. The angle brackets $\langle \dots \rangle$ denote a quantum-statistical average over the equilibrium state of an incoming single-mode channel not affected by the electron source. Such an equilibrium state is the Fermi sea with a temperature θ and a chemical potential μ . The other incoming channel of the wave splitter is in the same equilibrium state, with the same temperature θ and the same chemical potential μ .

For convenience, let us analyze this quantity in frequency representation. In the general nonstationary case, the current correlation function P_{34} depends on two frequencies. In the case with periodic driving, the Floquet scattering theory calculations give for our setup [81,82]:

$$P_{34}(\omega, \omega') = 2\pi \sum_{\ell=-\infty}^{\infty} \delta(\omega + \omega' - \ell\Omega) \mathcal{P}_{34,\ell}(\omega), \quad (\text{A3})$$

where the noise power $\mathcal{P}_{34,\ell}(\omega)$ is expressed in terms of the Floquet scattering matrix elements of an electron source, S_F , as follows:

$$\begin{aligned} & \mathcal{P}_{34,\ell}(\omega) \\ &= -RT \frac{e^2}{h} \int dE \sum_n \sum_m \sum_q f(E_q + \hbar\omega) f(E) \\ & \quad \times \{ \delta_{n0} \delta_{m+\ell,0} - S_F^*(E_n, E) S_F(E_{m+\ell}, E) \} \{ \delta_{nq} \delta_{mq} \\ & \quad - S_F^*(E_m + \hbar\omega, E_q + \hbar\omega) S_F(E_n + \hbar\omega, E_q + \hbar\omega) \}. \end{aligned} \quad (\text{A4})$$

Here n, m, q are integers, δ_{nm} is the Kronecker delta, and $f(E) = (1 + e^{\frac{E-\mu}{k_B\theta}})^{-1}$ is the Fermi distribution function for electrons in a metallic contact with temperature θ and chemical potential μ , k_B is the Boltzmann constant.

It's easy to see that in equilibrium, that is, when the source is turned off and, accordingly, $S_F(E_n, E_m) = \delta_{nm}$, the noise power is zero, $\mathcal{P}_{34,\ell}(\omega) = 0$. So, in our setup, where the contacts $\beta = 3$ and $\beta = 4$ have no direct connection between themselves, only the partition noise of injected particles, but not the quantum noise [83], contributes to the measured noise.

For convenience of the subsequent comparison with the electron correlation function, I represent the noise power as the sum of four terms, $\mathcal{P}_{34,\ell}(\omega) = -RT \frac{e^2}{h} \sum_{r=1}^4 B_r$, with

$$\begin{aligned} B_1 &= \int dE \sum_n \sum_m \sum_q f(E_q + \hbar\omega) f(E) \\ & \quad S_F^*(E_n, E) S_F(E_{m+\ell}, E) S_F^*(E_m + \hbar\omega, E_q + \hbar\omega) \\ & \quad S_F(E_n + \hbar\omega, E_q + \hbar\omega), \end{aligned} \quad (\text{A5a})$$

$$\begin{aligned} B_2 &= - \int dE \sum_q f(E_q + \hbar\omega) f(E) \\ & \quad S_F^*(E_q, E) S_F(E_{q+\ell}, E), \end{aligned} \quad (\text{A5b})$$

$$\begin{aligned} B_3 &= - \int dE \sum_q f(E_q + \hbar\omega) f(E) \\ & \quad S_F^*(E_{-\ell} + \hbar\omega, E_q + \hbar\omega) S_F(E + \hbar\omega, E_q + \hbar\omega), \end{aligned} \quad (\text{A5c})$$

$$B_4 = \delta_{\ell 0} \int dE f(E + \hbar\omega) f(E). \quad (\text{A5d})$$

Now let us turn to the quantum description of the excitations injected by the source.

2. Electron correlation function

As I discussed in Sec. II, the first-order correlation function for these excitations, $G^{(1)}$, is defined as the difference of the electron correlation functions with the source switched on and off, $G^{(1)}(t; t') = \langle \hat{\Psi}^\dagger(t) \hat{\Psi}(t') \rangle_{\text{on}} - \langle \hat{\Psi}^\dagger(t) \hat{\Psi}(t') \rangle_{\text{off}}$. Here $\hat{\Psi}(t)$ is a single-particle electron field operator in second quantization at time t just downstream the source. The angle brackets, $\langle \dots \rangle$, denote the quantum-statistical average over the state of the Fermi sea of electrons approaching the source from the metallic contact $\alpha = 1$ being in equilibrium. Note that, as in the Heisenberg picture, the field operators, rather than the state, are changed by a working source.

I adopt the wide band approximation and suppose that in the waveguides the electron spectrum can be linearized. The Floquet scattering theory expresses $G^{(1)}$ in terms of S_F as follows [32]:

$$\begin{aligned} & G^{(1)}(t; t') \\ &= \frac{1}{hv_\mu} \int dE f(E) e^{\frac{i}{\hbar} E(t-t')} \\ & \quad \times \left\{ \sum_{n,m=-\infty}^{\infty} e^{i\Omega(nt-mt')} S_F^*(E_n, E) S_F(E_m, E) - 1 \right\}. \end{aligned} \quad (\text{A6})$$

Note that the possibility to linearize an electron spectrum is important to perform linear opticlke manipulations with electrons. For instance, if we need to calculate $G^{(1)}$ at another place, say, at a distance x from the source downstream, we simply replace $t \rightarrow t - v_\mu x$ with v_μ being the Fermi velocity.

The wide band approximation is also crucial to get simple relations between electrical and quantum-mechanical quantities.

3. The connection between the two

Now let us demonstrate that the electrical noise power and the electron correlation function squared are related by the following Fourier transformation:

$$\frac{\mathcal{P}_{34,\ell}(\omega)}{P_0} = - \int_0^{T_0} e^{i\Omega t} dt \int_{-\infty}^{\infty} d\tau e^{i\omega\tau} |v_\mu G^{(1)}(t + \tau; t)|^2. \quad (\text{A7})$$

Here $\mathcal{P}_0 = e^2 RT/\mathcal{T}_0$ is the circuit constant. This constant is the shot noise caused by the scattering of single electrons being in the pure state on a wave splitter at a rate of one particle per period \mathcal{T}_0 [26].

The relation analogous to Eq. (A7) but for the zero-frequency noise power was presented in Refs. [32,42].

To prove Eq. (A7), first, let us represent the square of the correlation function, Eq. (A6), as the sum of four terms:

$$|v_\mu G^{(1)}(t; t')|^2 = \frac{1}{\hbar^2} \sum_{s=1}^4 A_s(t; t'), \quad (\text{A8a})$$

$$A_1(t; t') = \int dE f(E) e^{\frac{i}{\hbar} E(t-t')} \int dE' f(E') e^{\frac{-i}{\hbar} E'(t-t')} \sum_{n,m} e^{i\Omega(nt-mt')} S_F^*(E_n, E) S_F(E_m, E) \\ \times \sum_{j,k} e^{-i\Omega(jt-kt')} S_F(E'_j, E') S_F^*(E'_k, E'), \quad (\text{A8b})$$

$$A_2(t; t') = - \int dE f(E) e^{\frac{i}{\hbar} E(t-t')} \int dE' f(E') e^{\frac{-i}{\hbar} E'(t-t')} \sum_{n,m} e^{i\Omega(nt-mt')} S_F^*(E_n, E) S_F(E_m, E), \quad (\text{A8c})$$

$$A_3(t; t') = - \int dE f(E) e^{\frac{i}{\hbar} E(t-t')} \int dE' f(E') e^{\frac{-i}{\hbar} E'(t-t')} \sum_{j,k} e^{-i\Omega(jt-kt')} S_F(E'_j, E') S_F^*(E'_k, E'), \quad (\text{A8d})$$

$$A_4(t; t') = \int dE f(E) e^{\frac{i}{\hbar} E(t-t')} \int dE' f(E') e^{\frac{-i}{\hbar} E'(t-t')}. \quad (\text{A8e})$$

As the next step, let us perform the following Fourier transformation:

$$A_{s,\ell}(\omega) = \frac{1}{\hbar} \int_0^{\mathcal{T}_0} \frac{dt}{\mathcal{T}_0} e^{i\Omega\ell t} \int_{-\infty}^{\infty} d\tau e^{i\omega\tau} A_s(t + \tau, t), \quad (\text{A9a})$$

and show that $A_{s,\ell}(\omega)$ is nothing but B_s , Eqs. (A5).

Let us start with A_4 ,

$$A_{4,\ell}(\omega) = \frac{1}{\hbar} \int_0^{\mathcal{T}_0} \frac{dt}{\mathcal{T}_0} e^{i\Omega\ell t} \int_{-\infty}^{\infty} d\tau e^{i\omega\tau} \int dE f(E) e^{\frac{i}{\hbar} E\tau} \int dE' f(E') e^{\frac{-i}{\hbar} E'\tau} = \delta_{\ell 0} \int dE f(E) (E + \hbar\omega). \quad (\text{A9b})$$

This equation is exactly B_4 , Eq. (A5d).

The Fourier transform of A_3 , Eq. (A8d), gives us

$$A_{3,\ell}(\omega) = -\frac{1}{\hbar} \int_0^{\mathcal{T}_0} \frac{dt}{\mathcal{T}_0} e^{i\Omega\ell t} \int_{-\infty}^{\infty} d\tau e^{i\omega\tau} \int dE f(E) e^{\frac{i}{\hbar} E\tau} \int dE' f(E') e^{\frac{-i}{\hbar} E'\tau} \sum_{j,k} e^{-i\Omega j\tau} e^{-i\Omega t(j-k)} S_F(E'_j, E') S_F^*(E'_k, E') \\ = - \int dE \sum_j f(E) f(E_{-j} + \hbar\omega) S_F^*(E_{-\ell} + \hbar\omega, E_{-j} + \hbar\omega) S_F(E + \hbar\omega, E_{-j} + \hbar\omega). \quad (\text{A9c})$$

After replacing $-j$ by q we recognize the above equation as B_3 , Eq. (A5c).

The next term is A_2 , Eq. (A8c),

$$A_{2,\ell}(\omega) = -\frac{1}{\hbar} \int_0^{\mathcal{T}_0} \frac{dt}{\mathcal{T}_0} e^{i\Omega\ell t} \int_{-\infty}^{\infty} d\tau e^{i\omega\tau} \int dE f(E) e^{\frac{i}{\hbar} E\tau} \int dE' f(E') e^{\frac{-i}{\hbar} E'\tau} \sum_{n,m} e^{i\Omega n\tau} e^{i\Omega t(n-m)} S_F^*(E_n, E) S_F(E_m, E) \\ = - \int dE \sum_n f(E) f(E_n + \hbar\omega) S_F^*(E_n, E) S_F(E_{n+\ell}, E). \quad (\text{A9d})$$

This is the same as B_2 , Eq. (A5b).

And, finally, let us calculate the Fourier transform of A_1 , Eq. (A8b),

$$A_{1,\ell}(\omega) = \frac{1}{\hbar} \int_0^{\mathcal{T}_0} \frac{dt}{\mathcal{T}_0} e^{i\Omega\ell t} \int_{-\infty}^{\infty} d\tau e^{i\omega\tau} \int dE f(E) e^{\frac{i}{\hbar} E\tau} \int dE' f(E') e^{\frac{-i}{\hbar} E'\tau} \\ \times \sum_{n,m,j,k} e^{i\Omega(n-j)\tau} e^{i\Omega t(n+k-m-j)} \\ S_F^*(E_n, E) S_F(E_m, E) S_F(E'_j, E') S_F^*(E'_k, E') = \int dE \sum_{n,m,j} f(E) f(E_{n-j} + \hbar\omega) S_F^*(E_n, E) S_F(E_m, E) \\ \times S_F(E_n + \hbar\omega, E_{n-j} + \hbar\omega) S_F^*(E_{m-\ell} + \hbar\omega, E_{n-j} + \hbar\omega). \quad (\text{A9e})$$

We denote $q = n - j$ instead of j , and get

$$A_{1,\ell}(\omega) = \int dE \sum_q f(E) f(E_q + \hbar\omega) \sum_{n,m} S_F^*(E_n, E) S_F(E_m, E) S_F^*(E_{m-\ell} + \hbar\omega, E_q + \hbar\omega) S_F(E_n + \hbar\omega, E_q + \hbar\omega). \quad (\text{A9f})$$

After the shift $m - \ell \rightarrow m$, we find that this is nothing but B_1 , Eq. (A5a). Therefore, Eq. (A7) indeed holds.

The proof of Eq. (8) is completed.

4. The Fourier transformation for the product of first-order correlation functions

Here I show how the second term on the right-hand side of Eq. (9) is calculated from the corresponding term in Eq. (8) in the limit of $\mathcal{T}_0 \rightarrow \infty$.

The current generated by a periodically driven source is periodic in time, $I_\alpha(t) = I_\alpha(t + \mathcal{T}_0)$, $\alpha = 3, 4$. Therefore, we can expand it into the Fourier series,

$$I_\alpha(t) = \sum_{n=-\infty}^{\infty} e^{-in\Omega t} I_{\alpha,n},$$

$$I_{\alpha,n} = \int_0^{\mathcal{T}_0} \frac{dt}{\mathcal{T}_0} e^{in\Omega t}. \quad (\text{A10})$$

In the limit of $\mathcal{T}_0 \rightarrow \infty$, we introduce a continuous frequency $\omega_n = n\Omega$, replace $\sum_{n=-\infty}^{\infty} \rightarrow \int d\omega_n/\Omega$, and introduce the continuous Fourier transformation,

$$I_\alpha(\omega_n) = \int_{-\infty}^{\infty} dt e^{i\omega_n t} I_\alpha(t),$$

$$I_\alpha(t) = \int_{-\infty}^{\infty} \frac{d\omega_n}{\Omega} e^{-i\omega_n t} I_\alpha(\omega_n). \quad (\text{A11})$$

$$\frac{\mathcal{P}_{34,\ell}(\omega)}{\mathcal{P}_0} = - \int_0^{\mathcal{T}_0} dt e^{i\Omega t} \int_{-\infty}^{\infty} d\tau e^{i\omega\tau} |v_\mu G_{N=2}^{(1)}(t + \tau; t)|^2 = - \frac{\Gamma_\tau^2}{\pi^2} \int_0^{\mathcal{T}_0} dt e^{i\Omega t} \int_{-\infty}^{\infty} d\tau e^{i\omega\tau} \eta^2\left(\frac{\tau}{\tau_\theta}\right) \times \left\{ 2 \frac{1}{(t + \tau)^2 + \Gamma_\tau^2} \frac{1}{t^2 + \Gamma_\tau^2} + \frac{1}{(t + \tau - i\Gamma_\tau)^2} \frac{1}{(t + i\Gamma_\tau)^2} + \frac{1}{(t + \tau + i\Gamma_\tau)^2} \frac{1}{(t - i\Gamma_\tau)^2} \right\}. \quad (\text{B2a})$$

In the case when the levitons created at different periods do not overlap, $\mathcal{T}_0 \gg \Gamma_\tau$, we can safely extend the limits of integration over t to infinity and introduce a continuous frequency $\omega_\ell = \ell\Omega$ instead of the set of discrete frequencies $\ell\Omega$. Then, to integrate over t , we use the following auxiliary integrals:

$$2 \frac{\Gamma_\tau^2}{\pi^2} \int_{-\infty}^{\infty} dt \frac{e^{i\omega_\ell t}}{(t + \tau)^2 + \Gamma_\tau^2} \frac{1}{t^2 + \Gamma_\tau^2} = 2 \frac{\Gamma_\tau}{\pi} \frac{e^{-|\omega_\ell|\Gamma_\tau}}{\tau^2 + 4\Gamma_\tau^2} \begin{cases} 1 + e^{-i\omega_\ell\tau} - i \frac{2\Gamma_\tau}{\tau} (1 - e^{-i\omega_\ell\tau}), & \ell > 0, \\ 1 + e^{-i\omega_\ell\tau} + i \frac{2\Gamma_\tau}{\tau} (1 - e^{-i\omega_\ell\tau}), & \ell < 0, \end{cases} \quad (\text{B2b})$$

and

$$\frac{\Gamma_\tau^2}{\pi^2} \int_{-\infty}^{\infty} dt \frac{e^{i\omega_\ell t}}{(t + \tau - i\Gamma_\tau)^2} \frac{1}{(t + i\Gamma_\tau)^2}$$

$$= \frac{\Gamma_\tau^2}{\pi^2} \frac{e^{-|\omega_\ell|\Gamma_\tau}}{(\tau^2 + 4\Gamma_\tau^2)^2} \begin{cases} e^{-i\omega_\ell\tau} \left[-2\pi\omega_\ell(\tau^2 - 4\Gamma_\tau^2 + 4i\Gamma_\tau\tau) + \frac{4\pi(8\Gamma_\tau^3 - 6\Gamma_\tau\tau^2) + 4\pi i(\tau^3 - 12\Gamma_\tau^2\tau)}{\tau^2 + 4\Gamma_\tau^2} \right], & \ell > 0, \\ 2\pi\omega_\ell(\tau^2 - 4\Gamma_\tau^2 + 4i\Gamma_\tau\tau) + \frac{4\pi(8\Gamma_\tau^3 - 6\Gamma_\tau\tau^2) + 4\pi i(\tau^3 - 12\Gamma_\tau^2\tau)}{\tau^2 + 4\Gamma_\tau^2}, & \ell < 0. \end{cases} \quad (\text{B2c})$$

The noise power becomes

$$\frac{\mathcal{P}_{34,\ell}(\omega)}{\mathcal{P}_0} = -e^{-|\omega_\ell|\Gamma_\tau} \frac{2\Gamma_\tau}{\pi} \int_{-\infty}^{\infty} d\tau \frac{\eta^2\left(\frac{\tau}{\tau_\theta}\right)}{\tau^2 + 4\Gamma_\tau^2} \left\{ e^{i\omega\tau} + e^{i\tau(\omega - \omega_\ell)} - i \frac{2\Gamma_\tau}{\tau} \text{sgn}(\omega_\ell) [e^{i\omega\tau} - e^{i\tau(\omega - \omega_\ell)}] + \frac{e^{i\tau(\omega - \omega_\ell)} A + e^{i\omega\tau} A^*}{\tau^2 + 4\Gamma_\tau^2} \right\},$$

$$A = \Gamma_\tau |\omega_\ell| (4\Gamma_\tau^2 - \tau^2) - i 4\Gamma_\tau^2 \omega_\ell \tau + 2\Gamma_\tau \frac{(8\Gamma_\tau^3 - 6\Gamma_\tau\tau^2) + i \text{sgn}(\omega_\ell)(\tau^3 - 12\Gamma_\tau^2\tau)}{\tau^2 + 4\Gamma_\tau^2}. \quad (\text{B2d})$$

Then we use the second line of the above equation in Eq. (8) and get the corresponding term in Eq. (9).

APPENDIX B: THE FOURIER TRANSFORM OF THE FUNCTION $G^{(2)}$ FOR A TWO-ELECTRON LEVITON

The first-order correlation function of a two-electron leviton, $G_{N=2}^{(1)}$, is given in Eqs. (11) and (12) for $N = 2$. The corresponding second-order correlation function reads

$$G_{N=2}^{(2)}(t + \tau, t; t, t + \tau)$$

$$= -|G_{N=2}^{(1)}(t + \tau; t)|^2 + G_{N=2}^{(1)}(t; t) G_{N=2}^{(1)}(t + \tau; t + \tau). \quad (\text{B1})$$

Now let us apply the Fourier transformation defined in Eq. (A7).

1. The first term

The Fourier transform of the first term on the right-hand side of Eq. (B1) determines the finite-frequency noise power,

This equation satisfies the general symmetry properties, $\mathcal{P}_\ell(\omega) = \mathcal{P}_{-\ell}^*(-\omega)$ and $\mathcal{P}_\ell(\omega) = \mathcal{P}_\ell(\ell\Omega - \omega)$ [84]. To prove the latter one, we need to change $\tau \rightarrow -\tau$. Moreover, it's easy to see, that Eq. (B2d) is real:

$$\begin{aligned} \frac{\mathcal{P}_{34,\ell}(\omega)}{\mathcal{P}_0} &= -e^{-|\omega_\ell|\Gamma_\tau} \frac{4\Gamma_\tau}{\pi} \int_0^\infty d\tau \frac{\eta^2\left(\frac{\tau}{\tau_0}\right)}{\tau^2 + 4\Gamma_\tau^2} \{B[\cos(\omega\tau) + \cos([\omega - \omega_\ell]\tau)] + C[\sin(\omega\tau) - \sin([\omega - \omega_\ell]\tau)]\}, \\ B &= 1 + \Gamma_\tau |\omega_\ell| \frac{4\Gamma_\tau^2 - \tau^2}{\tau^2 + 4\Gamma_\tau^2} + 4\Gamma_\tau^2 \frac{4\Gamma_\tau^2 - 3\tau^2}{(\tau^2 + 4\Gamma_\tau^2)^2}, \\ C &= \frac{2\Gamma_\tau}{\tau} \text{sgn}(\omega_\ell) - 4\Gamma_\tau^2 \frac{\omega_\ell \tau}{\tau^2 + 4\Gamma_\tau^2} + 2\Gamma_\tau \text{sgn}(\omega_\ell) \frac{\tau^3 - 12\Gamma_\tau^2 \tau}{(\tau^2 + 4\Gamma_\tau^2)^2}. \end{aligned} \quad (\text{B2e})$$

Note the above equation is the total cross-correlation noise power, not the excess noise power, which is more convenient in the case of the auto-correlation noise measurement, see, e.g., Ref. [24].

The noise power $\mathcal{P}_{34,\ell}$, Eq. (B2e), vanishes at large frequencies, $\omega, \omega_\ell \gg \Gamma_\tau^{-1}$. This fact tells us that quantum noise[83], which grows with frequency, is not manifested here.

2. The second term

I denote the Fourier transform of the second line of Eq. (B1) as $G^{(2),cl}$. Since this part survives at high temperatures, which is expected for the classical contribution, I introduce the superscript *cl*. This part is expressed in terms of the Fourier transform of a current, carried by the levitons, $I(t) = ev_\mu G_{N=2}^{(1)}(t; t)$, as follows:

$$G_\ell^{(2),cl}(\omega) = \frac{1}{e^2 v_\mu^2} \int_0^{\mathcal{T}_0} e^{i\Omega t} dt \int_{-\infty}^\infty d\tau e^{i\omega\tau} I(t) I(t + \tau). \quad (\text{B3a})$$

Then I use the periodicity condition and write, $I(t) = \sum_{n=-\infty}^\infty e^{-in\Omega t} I_n$. The above equation becomes

$$G_\ell^{(2),cl}(\omega) = \frac{2\pi \mathcal{T}_0}{e^2 v_\mu^2} \sum_{n=-\infty}^\infty \delta(\omega - n\Omega) I_n I_{\ell-n}. \quad (\text{B3b})$$

In the long period limit, when the levitons emitted at different periods do not overlap, I introduce a continuous frequency $\omega_n = n\Omega$ and replace the sum by the integra,

$$\sum_{n=-\infty}^\infty \rightarrow \int_{-\infty}^\infty \frac{d\omega_n}{\Omega}. \quad (\text{B3c})$$

Correspondingly, the coefficients of a discrete Fourier transformation are replaced by the coefficients of a continuous Fourier transformation, $I_n \rightarrow I(\omega_n)/\mathcal{T}_0$. Then Eq. (B3b) becomes

$$v_\mu^2 G_\ell^{(2),cl}(\omega) = \frac{\mathcal{T}_0^2}{e^2} I(\omega) I(\omega_\ell - \omega), \quad (\text{B3d})$$

with $I(\omega) = ev_\mu G_{N=2}^{(1)}(\omega)$ and $G_{N=2}^{(1)}(\omega) = 2e^{-|\omega|\Gamma_\tau}$.

According to Eq. (9), the sum of Eqs. (B2e) and (B3d) defines the Fourier transform of the second-order correlation function:

$$v_\mu^2 G_{N=2,\ell}^{(2)}(\omega) = \frac{\mathcal{P}_{34,\ell}(\omega)}{\mathcal{P}_0} + v_\mu^2 G_\ell^{(2),cl}(\omega). \quad (\text{B4})$$

The above function is what is plotted in Fig. 3.

- [1] J. Splettstoesser, M. Moskalets, and M. Büttiker, Two-Particle Nonlocal Aharonov-Bohm Effect from Two Single-Particle Emitters, *Phys. Rev. Lett.* **103**, 076804 (2009).
- [2] G. Haack, M. Moskalets, and M. Büttiker, Glauber coherence of single-electron sources, *Phys. Rev. B* **87**, 201302 (2013).
- [3] E. Bocquillon, V. Freulon, F. D. Parmentier, J.-M. Berroir, B. Plaçais, C. Wahl, J. Rech, T. Jonckheere, T. Martin, Ch. Grenier, D. Ferraro, P. Degiovanni, and G. Fève, Electron quantum optics in ballistic chiral conductors, *Ann. Phys.* **526**, 1 (2014).
- [4] C. Bäuerle, D. C. Glatthli, T. Meunier, F. Portier, P. Roche, P. Rouleau, S. Takada, and X. Waintal, Coherent control of single electrons: a review of current progress, *Rep. Prog. Phys.* **81**, 056503 (2018).
- [5] C. H. Bennett and D. P. DiVincenzo, Quantum information and computation, *Nature* **404**, 247 (2000).
- [6] M. D. Blumenthal, B. Kaestner, L. Li, S. P. Giblin, T. J. B. M. Janssen, M. Pepper, D. Anderson, G. A. C. Jones, and D. A.

- Ritchie, Gigahertz quantized charge pumping, *Nat. Phys.* **3**, 343 (2007).
- [7] G. Fève, A. Mahé, J.-M. Berroir, T. Kontos, B. Plaçais, D. C. Glatthli, A. Cavanna, B. Etienne, and Y. Jin, An on-demand coherent single-electron source, *Science* **316**, 1169 (2007).
- [8] B. Kaestner, V. Kashcheyevs, S. Amakawa, M. D. Blumenthal, L. Li, T. J. B. M. Janssen, G. Hein, K. Pierz, T. Weimann, U. Siegner, and H. W. Schumacher, Single-parameter nonadiabatic quantized charge pumping, *Phys. Rev. B* **77**, 153301 (2008).
- [9] A. Fujiwara, K. Nishiguchi, and Y. Ono, Nanoampere charge pump by single-electron ratchet using silicon nanowire metal-oxide-semiconductor field-effect transistor, *Appl. Phys. Lett.* **92**, 042102 (2008).
- [10] B. Roche, R. P. Riwar, B. Voisin, E. Dupont-Ferrier, R. Wacquez, M. Vinet, M. Sanquer, J. Splettstoesser, and X. Jehl, A two-atom electron pump, *Nat. Commun.* **4**, 1581 (2013).

- [11] J. Dubois, T. Jullien, F. Portier, P. Roche, A. Cavanna, Y. Jin, W. Wegscheider, P. Roulleau, and D. C. Glattli, Minimal-excitation states for electron quantum optics using levitons, *Nature* **502**, 659 (2013).
- [12] A. Rossi, T. Tanttu, K. Y. Tan, I. Iisakka, R. Zhao, K. W. Chan, G. C. Tettamanzi, S. Rogge, A. S. Dzurak, and M. Möttönen, An accurate single-electron pump based on a highly tunable silicon quantum dot, *Nano Lett.* **14**, 3405 (2014).
- [13] G. C. Tettamanzi, R. Wacquez, and S. Rogge, Charge pumping through a single donor atom, *New J. Phys.* **16**, 063036 (2014).
- [14] S. d'Hollosy, M. Jung, A. Baumgartner, V. A. Guzenko, M. H. Madsen, J. Nygård, and C. Schönberger, Gigahertz quantized charge pumping in bottom-gate-defined InAs nanowire quantum dots, *Nano Lett.* **15**, 4585 (2015).
- [15] D. M. T. van Zanten, D. M. Basko, I. M. Khaymovich, J. P. Pekola, H. Courtois, and C. B. Winkelmann, Single Quantum Level Electron Turnstile, *Phys. Rev. Lett.* **116**, 166801 (2016).
- [16] J. Gabelli, K. Thibault, G. Gasse, C. Lupien, and B. Reulet, Characterization and control of charge transfer in a tunnel junction, *Phys. Status Solidi B* **254**, 1600619 (2017).
- [17] A. Rossi, J. Klochan, J. Timoshenko, F. E. Hudson, M. Möttönen, S. Rogge, A. S. Dzurak, V. Kashcheyevs, and G. C. Tettamanzi, Gigahertz single-electron pumping mediated by parasitic states, *Nano Lett.* **18**, 4141 (2018).
- [18] D. F. Walls and G. J. Milburn, *Quantum Optics* (Springer-Verlag, Berlin, Heidelberg, 2008).
- [19] A. A. Houck, D. I. Schuster, J. M. Gambetta, J. A. Schreier, B. R. Johnson, J. M. Chow, J. Majer, L. Frunzio, M. H. Devoret, S. M. Girvin, and R. J. Schoelkopf, Generating single microwave photons in a circuit, *Nature* **449**, 328 (2007).
- [20] D. Bozyigit, C. Lang, L. Steffen, J. M. Fink, C. Eichler, M. Baur, R. Bianchetti, P. Leek, S. Filipp, M. P. da Silva, A. Blais, and A. Wallraff, Antibunching of microwave-frequency photons observed in correlation measurements using linear detectors, *Nature Physics* **7**, 154 (2010).
- [21] N. Maire, F. Hohls, B. Kaestner, K. Pierz, H. W. Schumacher, and R. J. Haug, Noise measurement of a quantized charge pump, *Appl. Phys. Lett.* **92**, 082112 (2008).
- [22] A. Mahé, F. D. Parmentier, E. Bocquillon, J.-M. Berroir, D. C. Glattli, T. Kontos, B. Plaçaïs, G. Fève, A. Cavanna, and Y. Jin, Current correlations of an on-demand single-electron emitter, *Phys. Rev. B* **82**, 201309(R) (2010).
- [23] M. Albert, C. Flindt, and M. Büttiker, Accuracy of the quantum capacitor as a single-electron source, *Phys. Rev. B* **82**, 041407(R) (2010).
- [24] F. D. Parmentier, E. Bocquillon, J.-M. Berroir, D. C. Glattli, B. Plaçaïs, G. Fève, M. Albert, C. Flindt, and M. Büttiker, Current noise spectrum of a single-particle emitter: Theory and experiment, *Phys. Rev. B* **85**, 165438 (2012).
- [25] M. Reznikov, R. de-Picciotto, M. Heiblum, D. C. Glattli, A. Kumar, and L. Saminadayar, Quantum shot noise, *Superlattices Microstruct.* **23**, 901 (1998).
- [26] Y. M. Blanter and M. Büttiker, Shot noise in mesoscopic conductors, *Phys. Rep.* **336**, 1 (2000).
- [27] E. Bocquillon, F. D. Parmentier, C. Grenier, J.-M. Berroir, P. Degiovanni, D. C. Glattli, B. Plaçaïs, A. Cavanna, Y. Jin, and G. Fève, Electron Quantum Optics: Partitioning Electrons One by One, *Phys. Rev. Lett.* **108**, 196803 (2012).
- [28] M. Moskalets, Two-electron state from the Floquet scattering matrix perspective, *Phys. Rev. B* **89**, 045402 (2014).
- [29] E. Thibierge, D. Ferraro, B. Roussel, C. Cabart, A. Marguerite, G. Fève, and P. Degiovanni, Two-electron coherence and its measurement in electron quantum optics, *Phys. Rev. B* **93**, 081302 (2016).
- [30] B. Roussel, C. Cabart, G. Fève, E. Thibierge, and P. Degiovanni, Electron quantum optics as quantum signal processing, *Phys. Status Solidi B* **254**, 1600621 (2017).
- [31] M. Büttiker, Edge-state physics without magnetic fields, *Science* **325**, 278 (2009).
- [32] M. Moskalets and G. Haack, Single-electron coherence: finite temperature versus pure dephasing, *Physica E (Amsterdam)* **75**, 358 (2016).
- [33] M. Moskalets, Single-particle emission at finite temperatures, *Low Temp. Phys.* **43**, 865 (2017).
- [34] M. Büttiker, H. Thomas, and A. Prêtre, Mesoscopic capacitors, *Phys. Lett. A* **180**, 364 (1993).
- [35] J. Gabelli, G. Fève, J.-M. Berroir, B. Plaçaïs, A. Cavanna, B. Etienne, Y. Jin, and D. C. Glattli, Violation of Kirchhoff's laws for a coherent RC circuit, *Science* **313**, 499 (2006).
- [36] J. Keeling, A. V. Shytov, and L. S. Levitov, Coherent Particle Transfer in an On-Demand Single-Electronsources, *Phys. Rev. Lett.* **101**, 196404 (2008).
- [37] C. Grenier, R. Hervé, G. Fève, and P. Degiovanni, Electron quantum optics in quantum hall edge channels, *Mod. Phys. Lett. B* **25**, 1053 (2011).
- [38] C. Grenier, R. Hervé, E. Bocquillon, F. D. Parmentier, B. Plaçaïs, J.-M. Berroir, G. Fève, and P. Degiovanni, Single-electron quantum tomography in quantum Hall edge channels, *New J. Phys.* **13**, 093007 (2011).
- [39] M. Moskalets, G. Haack, and M. Büttiker, Single-electron source: Adiabatic versus nonadiabatic emission, *Phys. Rev. B* **87**, 125429 (2013).
- [40] T. Jullien, P. Roulleau, B. Roche, A. Cavanna, Y. Jin, and D. C. Glattli, Quantum tomography of an electron, *Nature* **514**, 603 (2014).
- [41] M. Moskalets, High-temperature fusion of a multielectron leviton, *Phys. Rev. B* **97**, 155411 (2018).
- [42] M. Moskalets, Single-particle shot noise at nonzero temperature, *Phys. Rev. B* **96**, 165423 (2017).
- [43] M. Büttiker, Scattering Theory of Thermal and Excess Noise in Open Conductors, *Phys. Rev. Lett.* **65**, 2901 (1990).
- [44] P. Samuelsson, E. V. Sukhorukov, and M. Büttiker, Two-Particle Aharonov-Bohm Effect and Entanglement in the Electronic Hanbury Brown-Twiss Setup, *Phys. Rev. Lett.* **92**, 026805 (2004).
- [45] I. Neder, N. Ofek, Y. Chung, M. Heiblum, D. Mahalu, and V. Umansky, Interference between two indistinguishable electrons from independent sources, *Nature* **448**, 333 (2007).
- [46] D. T. McClure, L. DiCarlo, Y. Zhang, H. A. Engel, C. M. Marcus, M. P. Hanson, and A. C. Gossard, Tunable Noise Cross Correlations in a Double Quantum Dot, *Phys. Rev. Lett.* **98**, 056801 (2007).
- [47] M. Henny, S. Oberholzer, C. Strunk, T. Heinzel, K. Ensslin, M. Holland, and C. Schönberger, The Fermionic Hanbury Brown and Twiss experiment, *Science* **284**, 296 (1999).
- [48] W. D. Oliver, J. Kim, R. C. Liu, and Y. Yamamoto, Hanbury Brown and Twiss-type experiment with electrons, *Science* **284**, 299 (1999).
- [49] S. Oberholzer, M. Henny, C. Strunk, C. Schönberger, T. Heinzel, K. Ensslin, and M. Holland, The Hanbury Brown and

- Twiss experiment with fermions, *Physica E (Amsterdam)* **6**, 314 (2000).
- [50] R. Hanbury Brown and R. Q. Twiss, A test of a new type of stellar interferometer on sirius, *Nature* **178**, 1046 (1956).
- [51] M. Büttiker, Role of scattering amplitudes in frequency-dependent current fluctuations in small conductors, *Phys. Rev. B* **45**, 3807 (1992).
- [52] R. C. Liu and Y. Yamamoto, Nyquist noise in the transition from mesoscopic to macroscopic transport, *Phys. Rev. B* **50**, 17411 (1994).
- [53] G. B. Lesovik and L. S. Levitov, Noise in an Ac Biased Junction: Nonstationary Aharonov-Bohm Effect, *Phys. Rev. Lett.* **72**, 538 (1994).
- [54] M. H. Pedersen and M. Büttiker, Scattering theory of photon-assisted electron transport, *Phys. Rev. B* **58**, 12993 (1998).
- [55] J. Salo, F. Hekking, and J. P. Pekola, Frequency-dependent current correlation functions from scattering theory, *Phys. Rev. B* **74**, 125427 (2006).
- [56] A. Braggio, M. Carrega, D. Ferraro, and M. Sassetti, Finite frequency noise spectroscopy for fractional Hall states at $\nu = 5/2$, *J. Stat. Mech.* (2016) 054010.
- [57] N. Dittmann and J. Splettstoesser, Finite-frequency noise of interacting single-electron emitters: spectroscopy with higher noise harmonics, [arXiv:1805.03130](https://arxiv.org/abs/1805.03130).
- [58] R. Schoelkopf, P. Burke, A. Kozhevnikov, D. Prober, and M. Rooks, Frequency Dependence of Shot Noise in a Diffusive Mesoscopic Conductor, *Phys. Rev. Lett.* **78**, 3370 (1997).
- [59] L. DiCarlo, Y. Zhang, D. T. McClure, C. Marcus, L. N. Pfeiffer, and K. W. West, A system for measuring auto- and cross-correlation of current noise at low temperatures, *Rev. Sci. Instrum.* **77**, 073906 (2006).
- [60] E. Zakra-Bajjani, J. Ségala, F. Portier, P. Roche, D. C. Glattli, A. Cavanna, and Y. Jin, Experimental Test of the High-Frequency Quantum Shot Noise Theory in a Quantum Point Contact, *Phys. Rev. Lett.* **99**, 236803 (2007).
- [61] J. Dubois, T. Jullien, C. Grenier, P. Degiovanni, P. Roulleau, and D. C. Glattli, Integer and fractional charge Lorentzian voltage pulses analyzed in the framework of photon-assisted shot noise, *Phys. Rev. B* **88**, 085301 (2013).
- [62] B. Gaury and X. Waintal, Dynamical control of interference using voltage pulses in the quantum regime, *Nat. Commun.* **5**, 3844 (2014).
- [63] P. P. Hofer and C. Flindt, Mach-Zehnder interferometry with periodic voltage pulses, *Phys. Rev. B* **90**, 235416 (2014).
- [64] W. Belzig and M. Vanević, Elementary Andreev processes in a driven superconductor-normal metal contact, *Physica E (Amsterdam)* **75**, 22 (2016).
- [65] T. J. Suzuki, Coherent transport of levitons through the Kondo resonance, *Phys. Rev. B* **95**, 241302 (2017).
- [66] D. C. Glattli and P. Roulleau, Pseudorandom binary injection of levitons for electron quantum optics, *Phys. Rev. B* **97**, 125407 (2018).
- [67] L. S. Levitov, H. Lee, and G. B. Lesovik, Electron counting statistics and coherent states of electric current, *J. Math. Phys.* **37**, 4845 (1996).
- [68] D. A. Ivanov, H. W. Lee, and L. S. Levitov, Coherent states of alternating current, *Phys. Rev. B* **56**, 6839 (1997).
- [69] J. Keeling, I. Klich, and L. S. Levitov, Minimal Excitation States of Electrons in One-Dimensional Wires, *Phys. Rev. Lett.* **97**, 116403 (2006).
- [70] F. Ronetti, L. Vannucci, D. Ferraro, T. Jonckheere, J. Rech, T. Martin, and M. Sassetti, Crystallization of levitons in the fractional quantum Hall regime, *Phys. Rev. B* **98**, 075401 (2018).
- [71] C. Grenier, J. Dubois, T. Jullien, P. Roulleau, D. C. Glattli, and P. Degiovanni, Fractionalization of minimal excitations in integer quantum Hall edge channels, *Phys. Rev. B* **88**, 085302 (2013).
- [72] M. Moskalets, First-order correlation function of a stream of single-electron wave packets, *Phys. Rev. B* **91**, 195431 (2015).
- [73] D. C. Glattli and P. S. Roulleau, Method and device for phase modulation of a carrier wave and application to the detection of multi-level phase-encoded digital signals, WO Patent App. PCT/FR2016/050193 (2016); <https://www.google.com/patents/WO2016124841A1?cl=en>.
- [74] D. C. Glattli and P. Roulleau, Hanbury-Brown Twiss noise correlation with time controlled quasi-particles in ballistic quantum conductors, *Physica E (Amsterdam)* **76**, 216 (2016).
- [75] D. C. Glattli and P. S. Roulleau, Levitons for electron quantum optics, *Phys. Status Solidi B* **254**, 1600650 (2016).
- [76] B. J. van Wees, H. van Houten, C. W. J. Beenakker, J. G. Williamson, L. P. Kouwenhoven, D. van der Marel, and C. T. Foxon, Quantized Conductance of Point Contacts in a Two-Dimensional Electron Gas, *Phys. Rev. Lett.* **60**, 848 (1988).
- [77] D. A. Wharam, T. J. Thornton, R. Newbury, M. Pepper, H. Ahmed, J. E. F. Frost, D. G. Hasko, D. C. Peacock, D. A. Ritchie, and G. A. C. Jones, One-dimensional transport and the quantisation of the ballistic resistance, *J. Phys. C* **21**, L209 (1988).
- [78] M. Moskalets and M. Büttiker, Floquet scattering theory of quantum pumps, *Phys. Rev. B* **66**, 205320 (2002).
- [79] M. Moskalets and G. Haack, Heat and charge transport measurements to access single-electron quantum characteristics, *Phys. Status Solidi B* **254**, 1600616 (2016).
- [80] M. Büttiker, Scattering theory of current and intensity noise correlations in conductors and wave guides, *Phys. Rev. B* **46**, 12485 (1992).
- [81] M. Moskalets and M. Büttiker, Time-resolved noise of adiabatic quantum pumps, *Phys. Rev. B* **75**, 035315 (2007).
- [82] M. Moskalets, Noise of a single-electron emitter, *Phys. Rev. B* **88**, 035433 (2013).
- [83] C. W. Gardiner and P. Zoller, *Quantum Noise* (Springer, New York, 2000).
- [84] M. Moskalets and M. Büttiker, Heat production and current noise for single- and double-cavity quantum capacitors, *Phys. Rev. B* **80**, 081302(R) (2009).